

1 **Size-resolved cloud condensation nuclei concentration**
2 **measurements in the Arctic: two case studies from the**
3 **summer of 2008**

4 **J. Zábori¹, N. Rastak¹, Y. J. Yoon², I. Riipinen¹, J. Ström¹**

5 [1]{Department of Environmental Science and Analytical Chemistry, Stockholm University,
6 106 91 Stockholm, Sweden }

7 [2]{Korea Polar Research Institute, Incheon 406-840, Republic of Korea }

8 Correspondence to: J. Zábori (julia.zabori@aces.su.se)

9

10 **Abstract**

11 The Arctic is one of the most vulnerable regions affected by climate change. Extensive
12 measurement data are needed to understand the atmospheric processes governing this
13 vulnerability. Among these, data describing cloud formation potential are of particular
14 interest, since the indirect effect of aerosols on the climate system is still poorly understood.
15 In this paper we present, for the first time, size-resolved cloud condensation nuclei (CCN)
16 data obtained in the Arctic. The measurements were conducted during two periods in the
17 summer of 2008: one in June, and one in August, at the Zeppelin research station (78°54'N,
18 11°53'E) in Svalbard. Trajectory analysis indicates that during the measurement period in
19 June 2008, air masses predominantly originated from the Arctic, whereas the measurements
20 from August 2008 were influenced mid-latitude air masses. CCN supersaturation (SS) spectra
21 obtained on the 27 June, before size-resolved measurements were begun, and spectra from the
22 21 and 24 August, conducted before and after the measurement period, revealed similarities
23 between the two months. From the ratio between CCN concentration and the total particle
24 number concentration (CN) as a function of dry particle diameter (D_p) at a SS of 0.4%, the
25 activation diameter (D_{50}), corresponding to $CCN/CN = 0.50$, was estimated. D_{50} was found to
26 be 60 and 67 nm for the examined periods in June and August 2008, respectively.
27 Corresponding D_{50} hygroscopicity parameter (κ) values were estimated to be 0.4 and 0.3 for
28 June and August 2008, respectively. These values can be compared to hygroscopicity values
29 estimated from bulk chemical composition, where κ was calculated to be 0.5 for both June
30 and August 2008. While the agreement between the two months is reasonable, the difference

31 in κ between the different methods indicates a size-dependence in the particle composition,
32 which is likely explained by a higher fraction of inorganics in the bulk aerosol samples.

33

34 **1 Introduction**

35 The Arctic represents a region of special interest for atmospheric research because it is: i)
36 very sensitive to changes in radiative forcing owing to a direct feedback mechanism; ii)
37 expecting greater anthropogenic activity from increased shipping and natural resource
38 explorations in the near future and iii) yet poorly understood in terms of climate controlling
39 processes, largely due to the lack of observational data. One of the most significant
40 uncertainties in climate prediction is the role of clouds, and in particular, the influence of
41 anthropogenic activities on clouds. In general, clouds have the ability to both cool the surface
42 by reflecting incoming solar radiation back to space, or warm the surface by re-emitting long-
43 wave radiation back to the surface (Boucher et al., 2013). The formation of clouds is
44 dependent on the presence of excess water vapour in the air and on the presence of aerosol
45 particles having cloud condensation nuclei (CCN) properties. Such particles must have
46 sufficient size and hygroscopicity to act as sites for cloud droplet formation. In this study, two
47 short case studies are presented, based on observations conducted in June and August 2008 at
48 the Zeppelin station, Svalbard. These data complement the existing CCN and aerosol
49 measurements conducted in the Arctic, but for the first time the CCN properties here are
50 determined on-line as a function of dry particle size. Moore et al. (2011a) have provided a
51 brief literature review of CCN measurements in the Arctic; however, to set our study in the
52 context of other studies and to summarize the available information concerning Arctic CCN,
53 we also present a short literature overview, including some of the most recent studies. For
54 clarity, data are first grouped into land-based measurements, then measurements from ships
55 and followed by aircraft measurements.

56

57 **Ground-based measurements**

58 Shaw (1986) examined the CCN spectra of air masses characterized by Arctic haze during
59 January and February 1985 in central Alaska. The maximum supersaturation (SS) was found
60 to be around 0.33%, and the dominant CCN consisted of soluble particles at a concentration
61 of a few hundred per cm^{-3} , characterized by a rather large size of approximately 1 μm .

62 Silvergren et al. (2014) presented chemical and physical properties of aerosols collected at the
63 Zeppelin research station, Svalbard from September 2007 to August 2008. Hygroscopic
64 growth and cloud forming potential were examined on a monthly basis. From this, it was
65 shown that during the summer months, the SS has the greatest impact on the number of CCN.
66 As the aerosol sulphate and nitrate mass concentrations reached a maximum between March
67 and May, it was concluded that these months presented the most unfavourable cloud forming
68 properties of the entire year. From September to February, sea salt was present in the highest
69 mass concentrations. Both the growth factor and the values of the hygroscopicity parameter κ
70 ranging approx. between 0.7 and 1 were determined to be highest in October, which was
71 noted as the month with the most favourable cloud forming potential.

72

73 **Ship-based measurements**

74 Bigg & Leck (2001) reported the results from CCN measurements conducted on an icebreaker
75 at latitudes higher than 80°N, from 15 July to 23 September 1996. They observed CCN
76 concentrations between 1 and 1000 cm⁻³ at a SS of 0.25% over the measurement period.
77 Daily median CCN concentrations at the same SS were around 15–50 cm⁻³, and over the
78 course of a day, concentrations could vary by up to one order of magnitude. A decrease in
79 CCN concentration of approximately one order of magnitude was observed when air was
80 being transported from the open ocean to the pack ice. The authors suggested that this
81 occurred as a result of wet scavenging. However, after this 36 h-period, an increase in CCN
82 concentration was observed, which was thought to be related to local aerosol production from
83 bubble bursting occurring between the pack ice.

84 The results of CCN measurements conducted during three weeks in August and September
85 2008 on board the icebreaker ‘Oden’, which was drifting passively to the north of 87°N, are
86 presented by Martin et al. (2011). A mean SS of 0.10% resulted in a mean CCN concentration
87 of 14 ± 11 cm⁻³, which increased up to 47 ± 37 cm⁻³ for a mean SS of 0.73%. In general,
88 CCN closure within the measurement uncertainties was successful for SSs of 0.10%, 0.15%
89 and 0.20%, assuming an internally mixed aerosol with a nearly insoluble organic volume
90 fraction. However, the calculated CCN concentrations for SSs of 0.41% and 0.73%
91 overestimated the measured CCN concentrations; this is suggested to be a result of differing
92 chemical properties of different aerosol sizes.

94 **Aircraft measurements**

95 Hoppel et al. (1973) present results of aircraft measurements from February 1972 above
96 Alaska, approximately 160 km north of Fairbanks. A strong temperature inversion was
97 observed during the measurements, and an increase in CCN concentration, approximately
98 from 100 to 400 cm^{-3} , was recorded to accompany an altitude increase, from 1.75 km to 4 km.
99 Moreover, the increase of CCN concentration with an increase in SS was dependent on the
100 altitude of the measurements. At 4.3 km altitude, the CCN concentration increased
101 approximately from 50 cm^{-3} at 0.3% SS to 600 cm^{-3} at 1% SS. In contrast, at approximately
102 0.3 km above sea level, an increase of CCN concentration was observed approximately from
103 60 cm^{-3} at 0.3% SS to 100 cm^{-3} at 0.8% SS, but no further increase was seen up to a SS of
104 1%. Hoppel et al. (1973) suggested that these data may indicate the production of CCN in the
105 upper troposphere or in the stratosphere, followed by downward mixing into the lower
106 atmospheric layers.

107 CCN data from aircraft measurements conducted during April 1992 over the Arctic Ocean
108 were presented by Hegg et al. (1995). Measurements took place around 350 km from the
109 Alaskan coast between 0.03- and 4-km altitude; they show CCN concentration to vary
110 between 19.9 and 92.7 cm^{-3} , with a mean value of $47 \pm 19 \text{ cm}^{-3}$ measured at 1% SS. Hegg et
111 al. (1995) also observed an increase in CCN concentration with altitude up to 3 km, but note
112 that the data points above 3-km altitude are too sparse to reliably predict any trend. Below
113 1.6-km altitude the fraction of particles that act as CCN ranged between 0.002 and 0.38 with
114 an average of 0.15 ± 0.08 at 1% SS. No reliable CN data were obtained for altitudes higher
115 than 1.6-km due to a frozen valve. Hegg et al. (1995) concluded that their data are an
116 indication of particle production at higher altitudes compared to lower altitudes.

117 Results of aircraft measurements made during 11 flights over Alaska in June 1995 were
118 published by Hegg et al. (1996) and compared to measurements presented in Hegg et al.
119 (1995). This further study concluded that the fraction of activated particles is, on average,
120 approximately 0.10 at a SS of 1%. They therefore suggested that the number of smaller
121 particles is higher during June 1995 than in the spring of 1992.

122 Yum & Hudson (2001) presented vertical CCN profiles obtained at least 500 km north of the
123 Alaskan coast during a flight campaign in May 1998. They observed a clear increase in CCN

124 concentration with an increase in altitude when low stratus clouds were present. However,
125 under non-cloudy conditions, an increase in CCN concentration was only observed at heights
126 with an air pressure lower than 700 mbar. Average CCN concentrations measured at a SS of
127 0.8% were 257 ± 79 and $76 \pm 29 \text{ cm}^{-3}$ above and below the stratus cloud, respectively. In
128 contrast, the average CCN concentrations obtained at lower altitudes (comparable to the
129 measurements beneath the clouds) during non-cloudy flights was $250 \pm 41 \text{ cm}^{-3}$. The authors
130 proposed that the CCN concentrations in the low cloudy boundary layer are controlled by
131 cloud scavenging, resulting in a clearly altitude-dependent CCN density profile. Analyses of
132 CCN spectra were also conducted, using the formula $N = C \cdot SS^k$, where N is the CCN
133 concentration at a given SS, C is the CCN concentration at 1% SS and k describes the slope of
134 the function. The CCN spectra at specific height levels showed larger k values under the non-
135 cloudy conditions, compared to when clouds were present (for example, 2.214 compared with
136 1.474 at 0.04%–0.1% SS and at 560–660 hPa), with the exception of the highest SS values
137 found at lower altitudes.

138 Moore et al. (2011a) presented results from five research flights over the Alaskan Arctic
139 during April 2008, beginning from Fairbanks and covering parts of the Beaufort Sea. The air
140 masses sampled variously represented background conditions, biomass burning plumes,
141 anthropogenic pollution and Arctic boundary layer conditions. Calculated activation curves
142 with SS values ranging between 0.1% and 0.6% showed that at least 70% of the particles were
143 activated for SS at around 0.2% for all air masses. It was therefore concluded that this
144 similarity in observed activation pattern, despite the differences in chemical composition, is a
145 result of aerosol size, which largely determines CCN activity. However, the authors pointed
146 out that for SS between 0.3% and 0.6% it is likely that the particle chemical composition
147 controls the maximum fraction of particles that can act as CCN.

148 Latham et al. (2013) presented results of CCN measurements conducted during research
149 flights from 26 June to 14 July 2008. The flight campaigns set-off from Cold Lake, Alberta,
150 Canada and passed through the northeastern Canadian Arctic before heading to the west coast
151 of Greenland. During the flights, the various air masses were characterized by biomass
152 burning, boreal forest background, Arctic background and anthropogenic industrial pollution.
153 Median CCN concentrations were highest for air masses influenced by fresh biomass burning,
154 at 7778 cm^{-3} at standard temperature and pressure (STP, 1013 hPa and 273.15 K). At a SS of
155 0.55% the CCN/CN ratio was around 0.89 for those particles resulting from fresh biomass

156 burning. The lowest CCN/CN activation ratio was 0.15 at SS 0.55%, observed for air masses
157 characterized by industrial pollution, with a CCN concentration of 341 cm^{-3} . The Arctic
158 background air mass resulted in a moderate activation ratio of 0.52 for 0.5% SS, while CCN
159 concentration was 247 cm^{-3} .

160 During a flight campaign over the northern slopes of Alaska in April 2008, Hiranuma et al.
161 (2013) collected ambient particles, dry residuals of mixed-phase cloud droplets and ice
162 crystals. They analysed their size and chemical structure using an electron microscope in
163 combination with various X-ray techniques. Note that the results should be interpreted with
164 caution due to the limited number of samples. However, the limited data showed that the
165 residuals of cloud droplets were enriched with respect to carbonate and black carbon,
166 compared to the ambient particles. Significant mixing was also observed in the cloud droplet
167 residuals. Additionally, during a period of high ice nucleation efficiency, residuals were
168 enriched in sodium and magnesium salts compared to the ambient particles.

169 The studies described above reveal the significant variability in CCN concentration across the
170 Arctic, likely resulting from differing locations of CCN production (upper troposphere vs.
171 lower boundary layer), production mechanisms, in-cloud processing and the origins of air
172 masses. Several studies indicate an increase in CCN with increasing altitude in the lower half
173 of the troposphere. However, the controlling mechanism for this increase is still unclear. In
174 this study, we compare bulk CCN properties with those found in previous studies, and we also
175 explore the size-dependence of CCN activation potential for the Arctic aerosols by combining
176 a DMPS (Differential Mobility Particle Sizer) system with a CCN counter (CCNC). Although
177 size dependent CCN activation has been studied worldwide (Bhattu & Tripathi, 2014; Rose et
178 al., 2010; Paramonov et al., 2013; Gunthe et al., 2009), according to our knowledge, this is the
179 first study presenting size-resolved CCN activation in the Arctic.

180

181 **2 Methods**

182 **2.1 Location**

183 Measurements were made at the Zeppelin research station ($78^{\circ}54'N$, $11^{\circ}53'E$, 474 m above
184 sea level), which is situated approximately 2 km south-west of the small settlement Ny-
185 Ålesund, in Svalbard. The station is seldom affected by local pollution and therefore can be
186 considered to represent remote Arctic atmospheric conditions. Continuous aerosol

187 measurements were begun in the year 2000, concerning which detailed information can be
188 found in Tunved et al. (2013).

189 **2.2 Instrumentation and experimental setup**

190 Particle number size distributions were measured using a closed-loop Differential Mobility
191 Particle Sizer (DMPS), consisting of a medium-sized Hauke Differential Mobility Analyzer
192 (DMA) in combination with a TSI Condensation Particle Counter (CPC) 3010. Measurements
193 were performed within 40 different size bins, with particle diameters ranging between 10 and
194 900 nm. Each particle size range was measured for 10 sec, followed by a lag time of 5 sec
195 before the next size range was measured. Simultaneously, total particle number
196 concentrations were precisely measured using a TSI CPC 3025 with a lower cut-off size of 3
197 nm, and by a TSI CPC 3010 with a lower cut-off size of 10 nm. A commercially available
198 DMT CCN counter connected to a 1/4" stainless steel tubing inlet registered CCN
199 concentrations at SSs of 0.2, 0.4, 0.6, 0.8 or 1 %."In the CCNC scanning mode, each SS level
200 was measured for approximately 5 min before changing to the next SS level. After completing
201 the 1% SS level, the measurements began again at 0.2% SS after at least a three min break in
202 the measurements. The shared inlet of the DMPS, TSI CPC 3025, and TSI CPC 3010 was
203 precipitation protected with an estimated cut-off size of 5 μm .

204 In the standard configuration these two instrument systems operate independently. In this
205 study, however, we combined the two systems such that the DMA first selects a nearly mono-
206 disperse aerosol, which is then supplied to the CCNC. For the CCN size-resolved
207 concentration measurements, the CCNC was connected to the DMA and SS was fixed at
208 0.4%. The number of size bins of the DMPS system was also reduced from 40 to 15, and the
209 time each particle size was measured was extended from 10 to 35 sec to improve counting
210 statistics. The lower and upper bounds of the DMPS scans were also narrowed to 15 and 400
211 nm, respectively. The two different setups of the CCNC are shown in Fig. 1.

212 **2.3 Experiments**

213 Two case studies are presented here, consisting of CCN size-resolved number concentration
214 measurements conducted during summer 2008. The measurement period for the first case
215 study lasted from around 9:40 on 27 June to around 10:15 on 29 June during which about 290
216 size-resolved CCN scans were conducted. The minimum and maximum temperatures for this

217 period were 3.8 and 9.4°C, respectively. The measurement period for the second case study
218 began at around 7:30 on 21 August and ended at around 10:50 on 24 August, resulting in
219 about 374 size-resolved CCN scans. The minimum and maximum temperatures for this period
220 were 2.8 and 5.9°C, respectively. Before the size-resolved CCN concentration measurements
221 were performed in June, CCN spectra were obtained from the total aerosols over a period of
222 approximately 5 h. Unfortunately, no spectra were measured directly after the first CCN size-
223 resolved experiment ended on 29 June. However, during the study in August, CCN spectra
224 were determined for approximately 17 h on 21 August, before the CCN size-resolved
225 experiment began, and for approximately 13 h on 24 August after the experiment ended. In
226 addition, 5-day backward trajectories were calculated on an hourly basis, using the online web
227 version of the NOAA HYSPLIT Model (Draxler & Rolph, 2014; Rolph, 2014), to analyse the
228 origins of the air masses from which the observed results presented in the next section were
229 derived.

230 **3 Results and Discussion**

231 **3.1 Time series analysis**

232 Particle number size distributions observed from 27 to 30 June 2008 are presented in Fig. 2a.
233 The vertical purple lines in this figure indicate the beginning and the end point of the
234 measurement period for the size-resolved CCN number concentration data. Based on the
235 particle number size distribution, at least three characteristic periods can be distinguished:
236 i) from midnight to approximately midday of 27 June, when particles with diameters of
237 approximately 70 nm dominate the particle concentration; ii) from midnight to approximately
238 midday of 28 June, when particle number concentrations are highest for particle diameters of
239 approximately 20 nm and iii) from approximately midday on the 29 of June to the following
240 midnight, when the concentration of particles with diameters approximately between 20 and
241 70 nm increased to more than 1000 cm⁻³ (cf. Fig. 2a). For the period 27 to 29 June, 5-day
242 backward trajectories were calculated for each hour (shown above Fig.2a and below Fig 2b).
243 Air masses arriving between 0:00 and 11:00 at Zeppelin station are characterized by both, air
244 coming from a southerly direction and air having its residence time exclusively at the high
245 Arctic. From 12:00 on the 27 of June until midnight of the 29 of June air masses reaching
246 Zeppelin station have a clear central Arctic origin. In addition to the trajectory analyses, Lidar
247 measurements from Ny-Ålesund, part of the Micro Pulse Lidar Network

248 (<http://mplnet.gsfc.nasa.gov/>, accessed 28 November 2013) were investigated for the presence
249 of clouds or precipitation in the vicinity of the Zeppelin station. All times mentioned in these
250 data refer to Coordinated Universal Time. Lidar measurements on the 27 of June 2008 in Ny-
251 Ålesund showed only high clouds (altitude > 5 km), from approximately 9:00. Before 9:00,
252 cloud-free conditions predominated at the measurement site. High clouds and cloud-free
253 conditions alternated during 28 and 29 June 2008; therefore, Zeppelin station can be regarded
254 as cloud-free during this time (cf. Fig. 3).

255 The time series of particle number size distribution (Fig. 2a) is accompanied by two time
256 series of total aerosol number concentrations for particles having a lower cut-off size of 3 and
257 10 nm, respectively (Fig. 2b). Although particles smaller than 10 nm are unlikely to be CCN,
258 the combination of the two CPC instruments permit detection of particles that are a result of
259 recent new particle formation. The combination of 5-day backward trajectory analyses, Lidar
260 measurements, particle number size distributions and total aerosol concentration time series
261 gives a rounded picture of the conditions that prevailed during the experimental period.

262 The entire period from 27 to 30 June 2008 is characterized by a maximum of particle
263 concentrations occurring at particle diameters below 100 nm. This is in line with the results of
264 Tunved et al. (2013), who analysed long-term particle number size distributions at Zeppelin
265 station during the years 2000–2010. In their study, the authors concluded that the Arctic
266 summer aerosol number size distribution (June–August) is characterized by a dominance of
267 particles with diameters less than the accumulation diameter. It is proposed that these aerosols
268 are most likely formed within the Arctic itself. This explanation of local production agrees
269 with our calculated trajectories (Fig. 2), which show transport almost only within the Arctic.
270 In addition, the Lidar data from the period from 27 to 30 June 2008 does not indicate any
271 cloud processing of the aerosols in the lower atmosphere boundary layer at the measurement
272 site.

273 From midnight to approximately midday of 27 June, particles with diameters of
274 approximately 70 nm dominate the particle concentration. The associated trajectory plot (Fig.
275 2) indicates that this pattern may result from a mixture of air masses, originating from the
276 Norwegian Sea as well as from the Arctic Ocean.

277 During the early morning hours of 28 June 2008 a sharp increase in total particle number
278 concentration is observed (Fig. 2b). The highest concentration of particle numbers is found
279 for particles with dry diameters of less than 20nm (Fig. 2a), which points together with the

280 sharp increase in particle number concentration towards new particle formation during
281 previous hours. The process of particle formation is not yet fully understood (Komppula et al.,
282 2003; Yli-Juuti et al., 2011; Ortega et al., 2012), but sulphuric acid and organic compounds
283 have been found to be the key components (Riipinen et al., 2007; Kuang et al., 2008; Sipilä et
284 al. 2010; Kulmala et al., 2013). Most nucleation events take place during the daylight hours,
285 which indicates the importance of photochemistry in the nucleation process. However, at
286 some locations particle formation events are also observed at night when there is no ambient
287 light (Ortega et al., 2012). In Ny-Ålesund, the polar day lasts from around 18 April to 23
288 August; therefore, the measurements made herein during June 2008 lie within this daylight
289 period. Tunved et al. (2013) presented averaged diurnal particle number size distributions for
290 June, based on observations made during 2000–2010, and found that the concentrations of
291 particles with diameters less than 20nm predominantly begin to increase at around noon. Here
292 presented data indicate, that an increase of particle concentration occurred later in the day. In
293 the Arctic environment, it has been suggested that dimethyl sulphide plays an important role
294 as a condensing vapour for the nucleation process (Chang et al., 2011). Tunved et al. (2013)
295 stated that another requirement of particle nucleation in the Arctic is a low condensation sink,
296 which means a low concentration of particles in the accumulation mode. These authors
297 showed that the particle mass is strongly related to accumulated precipitation along the
298 transport path (cf. Figure 15 in Tunved et al., 2013), and that conditions are favourable for
299 new particle formation during the period of midnight sun. Integrated precipitation over the
300 five day duration was calculated for each hourly trajectory. Over all there was little
301 precipitation during the investigated periods with a median of less than 3.7 mm for the June
302 case and less than 1.7 mm for the August case. The maximum integrated precipitation is an
303 isolated event for a trajectory arriving 0600 on 27 June. For this trajectory the integrated
304 precipitation was 18.5 mm. From this we can conclude that recent precipitation within the last
305 five days was not likely a dominant factor in shaping the aerosol properties during transport.

306 From midday on 29 June 2008 until approximately 22:30 on that day, the total particle
307 number concentrations of particles with diameters greater than 3 nm increased approximately
308 from 400 cm^{-3} to 3860 cm^{-3} (Fig. 2b). The highest concentrations were found for particles
309 with diameters between 30 and 70 nm. A change in the height pattern of the trajectories is
310 seen between the midday of the 29 June and the following hours (Fig. 2). It seems that the air
311 masses' height is reduced and it is possible that this change in transport pattern resulted in

312 more moisture supply to the air mass which helped promote particle formation and growth
313 when the sun was at its highest.

314 To place the period in which the size-resolved CCN measurements were conducted in a long-
315 term context, the median of the total particle number concentration for particles with
316 diameters greater than 10 nm during this period is compared with the medians of the June data
317 for the years 2001–2010 (Tunved et al., 2013). The long-term data have a time resolution of 1
318 h, but around 9% of these data are missing or are of poor quality and are therefore not
319 considered in the calculation. The data are available within specific size distributions, and the
320 total number was calculated by integrating over the distinct size ranges. From 2001 to 2005
321 the lowest measured size was 17.8 and the largest was 707.9 nm. From 2006 to 2007 a size
322 bin with a lower measurement range of 13.8 nm was added. For 2008–2010 the size
323 distribution diameter range was again broadened, to range between 10 and 790 nm. The
324 calculations resulted in a median particle number concentration of 177 cm^{-3} for 2001–2010,
325 with a 25th percentile of 80 cm^{-3} and a 75th percentile of 339 cm^{-3} . The median values with
326 25th percentile and 75th percentile for the period during which our CCN size-resolved
327 measurements were conducted during June 2008 are 245, 195 and 292 cm^{-3} , respectively.
328 Although the median total particle number concentration is somewhat 40% higher than the
329 averaged June data from 2001 to 2010, it falls within the 75th percentile of the long term data.
330 This in combination with the low particle concentrations in the accumulation mode and the
331 occurrence of a nucleation event indicates that the case study data from June 2008 can be
332 regarded as relatively representative.

333 Particle number size distributions from 21 to 25 August 2008 are presented in Fig. 4a. In this
334 figure, the purple vertical lines indicate the start and end times for the CCN size-resolved
335 concentration measurements. Difficulties with the DMPS measurements occurred
336 approximately from 8:00 to 19:30 on 21 August and for short periods on 22 August; these
337 time periods are omitted from the analysis. The particle number size distribution time series
338 represent time series of total particle number concentrations with dry diameters greater than 3
339 and 10 nm, respectively (cf. Fig. 4b). As with the measurements from June 2008, different
340 periods with different characteristic particle number size distributions can be distinguished
341 during the studied time period in August 2008 (Fig. 4a): i) the final hours of 21 August, when
342 particle number concentrations were highest for particles with diameters between 100 and 200
343 nm; ii) the early morning hours of 23 August, when particle number concentrations were

344 relatively low for all measured sizes (cf. Fig. 4b) and iii) during the first half of 24 August,
345 when total aerosol concentrations were relatively high for the period, but no particular size
346 range clearly dominated. Calculated 5-day backward trajectories for each hour indicate that
347 air masses arriving on the 21 August at Zeppelin station mainly come from the southern part
348 of the Norwegian Sea (Fig. 4). Air masses arriving from the 22 August until midday the 24
349 August at Zeppelin station have a more northern origin, the Barents Sea Air masses arriving
350 between midday and midnight on the 24 of August at Zeppelin station have again an origin
351 over the Norwegian Sea.

352 As with the measurement period in June 2008, Lidar data were consulted to investigate any
353 local effects from clouds and precipitation (cf. Fig. 5). During the 21 August 2008, apparently
354 clouds are present approximately between 0.7 and 9 km above the Zeppelin station. However,
355 no precipitation reaching the station level could be detected. On 22 August low clouds
356 (altitude < 2 km) were observed from approximately 9:00, and precipitation started at
357 approximately 24:00, continuing until approximately 9:00. Only a few precipitation events are
358 observed on 23 August 2008 for the most part, no clouds are observed at the altitudes above
359 the Zeppelin station. On 24 August, clouds were only observed in Ny-Ålesund at altitudes
360 higher than 0.8 km.

361 From around 20:00 to 23:00 on 21 August 2008, particles with dry diameters between 100
362 and 200 nm dominate the particle number size distribution. During the time period of 2:00
363 and 24:00 on the 21 of August, the Zeppelin research station was according to the Lidar
364 measurements very likely unaffected by clouds. The trajectories of the 21 August show that
365 air masses originate from the mid-latitudes and lower their height when reaching Zeppelin
366 research station (Fig. 4). Therefore, it is likely that the peak in the particle number size
367 distribution for particles with diameters between 100 nm and 200 nm is a result of particles
368 being transported from the mid-latitudes to the Arctic and the processes taking place during
369 transport rather than particles are being produced locally. The accumulation mode-dominated
370 size distribution differs somewhat from the typical summer conditions. Tunved et al. (2013)
371 demonstrated from their long-term average, during June–August, which locally produced
372 particles with diameters in the nucleation and Aitken mode dominate the particle number size
373 distribution. In the morning hours of 23 August 2008, air masses arriving at Zeppelin station
374 originated in the Barents Sea (Fig. 4) and resulted in relatively low total particle
375 concentrations, compared to the concentrations observed between 20:00 and 23:00 on 21

376 August 2008 (Fig. 2b). Air masses in the morning of the 24 of August originated as well in
377 the Barents Sea, but result in higher total particle concentrations than observed on the 23 of
378 August.

379 To place our second case study data in a long-term context, we compare median values of
380 August 2008 with the 10-year climatology presented by Tunved et al. (2013). Approximately
381 12% of the hourly data were excluded from calculations of the median integrated particle
382 number concentration from 2001 to 2010 August, owing to them being either missing or of
383 poor quality. The calculations produced a median particle number concentration of 127 cm^{-3}
384 for August during 2001–2010, with a 25th percentile of 58 cm^{-3} and a 75th percentile of 252
385 cm^{-3} . In comparison, the median values with 25th percentile and 75th percentile for the size-
386 resolved CCN measurement period in August 2008 are 226, 147 and 329 cm^{-3} , respectively.
387 Although, the total particle number concentration during the period in which the CCN size-
388 resolved measurements were conducted is about 80 % higher than the long-term average, the
389 particle number concentration still falls within the 75th percentile.

390 Overall, the June case is similar to the long-term climatology and appears to be more
391 representative of the summer period, with air masses of Arctic origin. In contrast, the August
392 case differs more from the long-term climatology and shows a more significant influence of
393 lower latitudes and higher number densities of accumulation particles.

394 **3.2 CCN spectra**

395 A CCN spectrum for a 5 h-long period on the 27 June 2008 was obtained before the size-
396 resolved CCN measurements were begun. The data presented in this section comprise
397 medians calculated from one SS scanning cycle. The ratio, as function of SS, between CCN
398 number concentration and the total particle number concentrations for particles with diameters
399 greater than 3 nm ($\text{CN}_{>3\text{nm}}$) for 27 June 2008 is shown in Fig. 6a. A significant increase in the
400 ratio of CCN to CN with an increase in SS is detectable by applying the two-sample
401 Kolmogorov–Smirnov test, only for an increase in SS from 0.2% to 0.4%. The absolute
402 number of CCN dependent on SS is shown for 27 June 2008 in Fig. 6b. Applying the two-
403 sample Kolmogorov–Smirnov test to the data resulted in a significant difference in CCN
404 numbers with increasing SS (5% significance level). The power-law function, $N_{\text{CCN}}(\text{SS}) =$
405 $C \cdot \text{SS}^k$, describing the number of CCN (N_{CCN}) with the coefficients C and k and SS, was fitted
406 to the data shown in Fig. 6b and giving values for the coefficients of $C = 221$ and $k = 0.482$.

407 Ranges in the parameters C and k depend on the type of air mass, and the values for 27 June
408 2008 will be discussed in a later section, in combination with the values obtained from the
409 August 2008 data.

410 CCN spectra obtained during 17 h and 13 h observation periods on 21 and 24 August 2008,
411 respectively, are shown on the right side of Fig. 6. The ratios between CCN and CN as a
412 function of SS are shown in Fig. 6c for the two different days. For 21 August, a significant
413 increase in the CCN to CN ratio with an increase in SS was observed in all cases. For 24
414 August, the increase in ratio was significant for all increases in SS, except for the increase
415 from 0.4% to 0.6% SS. The absolute number of CCN for 21 and 24 August, as a function of
416 SS, is shown in Fig. 6d. For both days, the increase in CCN number from one SS to the next is
417 significant. This is based on applying the two-sample Kolmogorov–Smirnov test with a 5%
418 significance level. As with the same data from 27 June 2008 (cf. Fig. 6b), a power-law
419 function of the same form was fitted to the data from 21 and 24 August 2008, as denoted by
420 the red lines in Fig. 6d. The fittings resulted in $C = 251$ and $C = 146$ and $k = 0.367$ and $k =$
421 0.446 for 21 and 24 August 2008, respectively.

422 Rogers & Yau (1996) demonstrated that the coefficients for maritime air vary, with $C = 30$ –
423 300 cm^{-3} and $k = 0.3$ – 1.0 , while for continental air the values vary between $C = 300$ – 3000
424 cm^{-3} and $k = 0.2$ – 2.0 . The coefficients C and k that are given by the fitted power-law function
425 applied to the measurements during June and August 2008 (cf. Fig 6b and Fig. 6d) are
426 consistent with the ranges that Rogers & Yau (1996) proposed for maritime air masses.
427 Pruppacher & Klett (2010) also presented a compilation of C and k values from different
428 studies, alongside the CCN/CN ratio for a SS of 1% at different locations, characterized by
429 either maritime or continental air masses. Only one study from the Arctic, influenced by a
430 maritime air mass, is presented, providing a C value between 100 and 1000 cm^{-3} . Pruppacher
431 & Klett (2010) did not present a k value for this study, but stated that the CCN/CN at 1% SS
432 is 0.5. Compared to the data from Zeppelin in this study, this range is at the lower limit of that
433 observed on 21st August 2008, and at the upper limit of that observed on 27 June and 24
434 August 2008 (cf. Fig. 6a and Fig. 6c). However, it should be noted that direct comparison is
435 difficult as it is not known which size range was considered for the integrated number of CN.
436 Hegg et al. (1995) also presented a number of C and k values and CCN/CN ratios obtained
437 during several flight campaigns over the Arctic. Although an increase in CCN was observed
438 with an increase in altitude for a SS of 1%, CCN concentrations for altitudes $< 1.6 \text{ km}$ were

439 always lower than 100 cm^{-3} . This is in contrast to the measurements obtained at Zeppelin
440 station in this study, where CCN concentrations were generally higher than 100 cm^{-3} at a SS
441 of 1% (cf. Fig. 6b and Fig. 6c). The average CCN/CN ratio for measurements conducted at
442 altitudes lower than 1.6 km was calculated to be 0.15 (Hegg et al., 1995), which is lower than
443 the calculated average ratios of 0.32, 0.77 and 0.38 obtained for a SS of 1% for 27 June, 21
444 and 24 August 2008.

445 Yum & Hudson (2001) estimated an average CCN concentration of 76 cm^{-3} in conditions
446 when low clouds are present and an average of 250 cm^{-3} for non-cloudy conditions at a SS of
447 0.8%. Estimating the CCN concentration at 0.8% SS with the power-law function results in
448 CCN concentrations of 199 cm^{-3} , 231 and 132 cm^{-3} for 27 June, 21 and 24 August,
449 respectively. For 27 June only high clouds (altitude > 5 km) were present, while for 21 and 24
450 August clouds were observed at altitudes higher than 0.7 km (cf. Sect. 3.1). The CCN
451 concentrations calculated herein using the power law relation and a SS of 0.8% for June and
452 August clearly lies between those CCN concentrations determined by Yum & Hudson (2001)
453 for non-cloudy conditions. The CCN/CN ratio calculated by Yum & Hudson (2001) is 0.65 at
454 a SS of 0.8%, which is higher than the average ratio determined for the CCN spectra during
455 27 June and 24 August 2008. The arithmetic means of the CCN/CN ratio at a SS of 0.8% are
456 0.31, 0.75 and 0.35 for 27 June, 21 and 24 August 2008, respectively. Yum & Hudson (2001)
457 also present altitude-dependent k values for a SS range of 0.1%–0.6%. The k values for
458 cloudy conditions ranged between 0.27 and 0.55 and between 0.34 and 0.75 for non-cloudy
459 conditions. Calculated k values for 27 June, 21 and 24 August 2008, only considering a SS
460 range of 0.2% to 0.6%, were found to be 0.65, 0.41 and 0.37, which is similar to the results
461 obtained by Yum & Hudson (2001).

462 Silvergren et al. (2014) presented CCN number concentrations as a function of SS and as a
463 function of the month from September 2007 to August 2008, calculated based on aerosol
464 collections on filters at Zeppelin research station. For June 2008, a CCN number
465 concentration of around 100 cm^{-3} at a SS of 0.4% is shown. This concentration is lower than
466 the calculated CCN number concentration found here using the power-law relation shown in
467 Fig. 6 and a SS of 0.4%, which results in a CCN number concentration of 142 cm^{-3} . For
468 August 2008, Silvergren et al. (2014) calculated a CCN number concentration of
469 approximately 65 cm^{-3} at 0.4 % SS for the Zeppelin research station, which is although lower

470 than the concentrations of 179 and 97 particles cm^{-3} calculated from the presented data in Fig.
471 6d for 21 and 24 August 2008.

472 No clear separation can be made between the two CCN spectra from August 2008 and the one
473 CCN spectrum from June 2008. In general, the CCN spectrum of June 2008 (Fig. 6b) lies
474 between the two different spectra of August 2008 (Fig. 6d). Comparing backward trajectories
475 arriving at Zeppelin before midday the 27 June (Fig. 2) and before midday the 21 August and
476 after midday the 24 August (Fig. 4), corresponding to the times when the CCN spectra were
477 measured, show that the air masses' origin was for the most of the times southerly of
478 Svalbard. However, even those air masses with similar origins can show differences in their
479 aerosol characteristics (Park et al., 2014).

480 **3.3 CCN activation diameter**

481 The size-resolved activation of particles having D_p between 15 and 400 nm at 0.4% SS is
482 shown in Fig. 7. The upper panel shows the geometric mean of the activated particle
483 concentration measured by the CCNC compared to the geometric mean of the total particle
484 (CN) concentration measured by the CPC for the measurement period during June 2008
485 (Fig.7a). The lower panel shows the correspondent data for the measurement period in August
486 2008 (Fig. 7b). The most distinct differences between the particle number concentrations of
487 total particles measured by the CPC during the experimental period in June 2008 and August
488 2008 is a) a higher particle number concentration having $D_p < 20$ nm during June; b) a peak of
489 particle concentration at approximately D_p 50 nm in August and c) a higher variation in
490 particle concentration for the different size bins indicated by a higher geometric SD during
491 August compared to June. As the CN number concentration, the CCN concentration is
492 characterized by a higher variability during the measurement period in August compared to
493 the measurement period in June.

494 To establish the presented study contextually with other studies, the ratio between CCN and
495 CN as a function of dry particle diameter was calculated (Fig. 8). Note that during June the
496 CCN concentration exceeds the total particle concentration for $D_p > 156$ nm, and during
497 August the CCN concentration is higher than the CN concentration for $D_p < 19$ nm and $D_p >$
498 123 nm. The experimental approach of selecting a narrow size range that can be applied to the
499 CCNC results in very low particle concentrations in the instrument. In particular, for
500 measurements made at either end of the size distribution, small errors can cause large changes

501 in the ratio, as presented in Fig. 8. To obtain completeness, all data points are shown;
502 however, the sizes where $CCN/CN \geq 1$ have been shaded and disregarded.

503 After applying a spline interpolation to the measurement data, the dry diameter at which 50%
504 of the total particle number concentration was activated (D_{50}) was calculated to be 60 nm for
505 the measurement period in June 2008 and 67 nm in August 2008. To the best of our
506 knowledge, to date no size-resolved CCN measurements in the Arctic have been published;
507 therefore, data are compared to results obtained in the subarctic. Anttila et al. (2012) reported
508 a study that was conducted at the Finnish Pallas-Sodankylä Global Atmospheric Watch
509 station that measured the ratio between cloud droplet number concentration and total particle
510 concentration while the station was in clouds as a function of dry particle size. By comparing
511 CCN concentrations at a fixed SS of 0.4% with cloud droplet number concentrations, it was
512 concluded that during the cloud events the “effective” maximal SS was likely to be
513 approximately 0.4% in most cases. During the five periods when the station was in clouds,
514 D_{50} varied between 80 and 102 nm on average. A comparable study at the same measurement
515 site resulted in D_{50} between 110 and 140 nm for maximal SS between 0.18% and 0.26%
516 (Anttila et al., 2009). Komppula et al. (2005) calculated D_{50} by comparing a particle number
517 size distribution measured at a site in clouds with a nearby measured size distribution
518 obtained at a station under cloud-free conditions. D_{50} was estimated to be 80 nm on average
519 and varied between 50 and 128 nm. Unfortunately, the SS is unknown. Due to the uncertainty
520 in SS, it is not possible to compare present study to the studies conducted at the Finnish
521 stations directly. However, due to SS lower than 0.4% reported by Anttila et al. (2012) and
522 Anttila et al. (2009), larger activation diameters in these studies compared to this study are
523 expected, which is in line with the presented results. Jaatinen et al. (2014) report activation
524 diameters for measurements conducted during the same field campaign as reported in Anttila
525 et al. (2012). However, compared with Anttila et al. (2012), in the present study, activation
526 diameters were calculated differently and for a shorter period. The critical diameter was
527 calculated by interpolating between the size bin at which the integrated particle number size
528 distribution was equal to the amount of total measured CCN and the previous size bin. This
529 resulted in a critical diameter of 98 ± 16 nm for 0.4% SS (Jaatinen et al., 2014).

530 Besides SS, the chemical composition and mixing state determines the ability of particles to
531 become activated to cloud droplets (Frosch et al. 2011; Moore et al., 2011b; Ervens et al.,
532 2010; Sullivan et al., 2009). Kreidenweis et al. (2005) summarize results of predicted and

533 experimentally determined critical diameters of ammonium sulphate and sodium chloride
 534 particles. Predicted critical diameters for sodium chloride particles vary between 44.6 and
 535 39.4 nm (Kreidenweis et al., 2005 and references therein) and the experimentally determined
 536 diameter for a SS of 0.4% was reported to be 40 ± 6 nm (Corrigan & Novakov, 1999 in
 537 Kreidenweis et al. 2005). Ammonium sulphate particles had larger predicted activation
 538 diameters at SS of 0.4%, i.e., from 62.6 to 49 nm (Kreidenweis et al., 2005 and references
 539 therein). Experimentally determined critical diameters of ammonium sulphate were 51 ± 8
 540 and 59 ± 9 nm (Corrigan & Novakov, 1999 and Kumar et al., 2003 in Kreidenweis et al.,
 541 2005). Corrigan and Novakov (1999) experimentally estimated D_{50} measured at a SS of 0.4%
 542 to be 82 nm, 148 and 74 nm for succinic acid, adipic acid and glucose aerosols, respectively.
 543 It was concluded that all D_{50} match well with the D_{50} calculated theoretically, except for the
 544 less soluble adipic acid. Kumar et al. (2003) experimentally determined the activation
 545 diameter of oxalic acid to be 65 nm at a SS of 0.40%. In the following section, the obtained
 546 information of the activation diameter, as well as the chemical information about the aerosol
 547 at the Zeppelin research station from another study are used to calculate the hygroscopicity
 548 parameter κ .

549 **3.4 Comparison of κ values obtained with different methods**

550 The hygroscopicity parameter κ was first introduced by Petters and Kreidenweis (2007) to
 551 describe the relationship between particle dry diameter and CCN activity. In this study, κ
 552 values were calculated with two independent approaches for June and August 2008: 1) based
 553 on the CCN activation of the aerosol population; 2) based on the bulk chemical composition
 554 of the particulate mass sampled at the site.

555 First, the relationship between the activation diameter ($D_{p,act}$) and SS derived from κ -Köhler
 556 theory (Asa-Awuku et al., 2010) was applied to the experimental CCN data:

$$557 \quad SS = \frac{2}{3} \left[\frac{4M_w \sigma}{RT\rho} \right]^{3/2} (3\kappa D_{p,act}^3)^{-1/2}. \quad (1)$$

558 where M_w (kg mol^{-1}) is the molar mass of water, T is the temperature, R is the universal molar
 559 gas constant, σ is the surface tension of the solution/air interface and ρ (kg m^{-3}) is the density
 560 of the solution. The surface tension of pure water 0.072 J m^2 and the density of pure water
 561 1000 kg m^{-3} were applied. Temperature was assumed to be 295 K to match the temperature in
 562 the instruments. When analysing the experimental data, the activation diameter was assumed

563 to be the dry diameter corresponding to the CCN to CN ratio of 0.5. However, we tested the
564 sensitivity to this assumption by repeating the calculations for CCN/CN values of 0.25 and
565 0.75. The resulting κ values were 0.2–0.7 for June and 0.2–0.5 for August, with the best
566 estimates (corresponding to the 50%-points in the CCN/CN ratios) of 0.4 and 0.3, respectively
567 (Table 1).

568 Second, the κ values derived from the CCN activation data were compared to κ values
569 obtained using the aerosol composition data. In this case, the total κ for the multi-component
570 aerosol particles was calculated using the simple mixing rule

$$571 \quad \kappa = \sum_i \varepsilon_i \kappa_i \cdot \quad (2)$$

572 where ε_i and κ_i are the volume fraction and hygroscopicity parameter of each component i ,
573 respectively (Petters & Kreidenweis, 2007). We assumed internally mixed aerosol particles,
574 composed of four surrogate components (inorganics, more water-soluble organics, less water-
575 soluble organics and elemental carbon, similar to Rastak et al., 2014; see Table 2 for the
576 assumed single-component properties). The monthly mass fractions of the organic
577 components were estimated by analysing filter samples of particles that passed a PM₁₀ inlet.
578 The inorganic fraction was determined after sampling the aerosol with an open face system
579 without a PM₁₀ inlet but shielded with a cylinder that reduced the sampling efficiency for
580 particles larger than 10 μm (Silvergren et al., 2014). It should be noted that the properties of
581 ammonium sulphate were used to describe the inorganic fraction. The sea salt contribution in
582 the inorganic fraction was not considered for particles less than 400 nm (upper bound of the
583 DMPS in this study). The resulting total κ values were approximately 0.5 for both considered
584 months (Table 2).

585 Comparison of the “bulk κ ” (obtained with Eq. (2) and bulk chemical composition) with the
586 “CCN κ ” (obtained from the CCN/CN = 0.50 point with Eq. (1)) shows reasonable agreement
587 for June but a slight overestimation for August. This could be due to the overestimation of the
588 inorganic fraction in the “bulk κ ”, as particles with diameters >400 nm were also able to reach
589 the filter. The chemical composition was therefore probably not accurately representative of
590 the CCN-sized particles. In addition, it should be noted that the data used to calculate κ with
591 Eq. (1) are based on only 2–3 days of measurements during June and August 2008 while the
592 calculations used in Eq. (2) are based on bulk aerosol properties over the whole month of June
593 and August 2008.

594 Silvergren et al. (2014) used three different approaches to calculate κ for June 2008 and
595 August 2008. Bulk aerosol samples on filters were obtained during June and August 2008 at
596 the Zeppelin research station. The filters were extracted and the extract was again filtered so
597 that only the water-soluble fraction of the aerosols remained. With the first two approaches,
598 particles were generated by an atomizer and then measured in a Hygroscopic Tandem
599 Differential Mobility Analyser (HTDMA) and a CCNC. The corresponding κ values were
600 calculated based on determined growth factors and critical SS and were estimated to be
601 approximately between 0.4 and 0.5 on an average for both June and August 2008. In the third
602 method, Silvergren et al. (2014) used the chemical information from the filter samples in
603 combination with literature values to determine the activation diameter and the critical SS
604 based on Köhler theory. The resulting κ values were approximately 0.7 for both June and
605 August 2008 (cf. Fig. 9 in Silvergren et al., 2014). In present study, the “CCN κ ” value for
606 June was 0.4, which is in the lower end of results reported by Silvergren et al. (2014). For
607 August, “CCN κ ” was 0.3, which is lower than the results presented by Silvergren et al.
608 (2014). The “bulk κ ” values determined here are within the ranges determined by Silvergren
609 et al. (2014) based on HTDMA and CCNC measurements.

610 Based on aerosol optical properties, Zieger et al. (2010) determined a mean κ value of 0.6 for
611 the period July to October 2008 at the Zeppelin research station. The value presented by
612 Zieger et al. (2010) is somewhat higher than the “bulk κ ” estimated in this study (0.5 for both
613 months). Conversely, the κ values calculated from the D_{50} using the DMPS-CCNC
614 combination are clearly lower (0.4 for June, and 0.3 for August).

615 The main reason for the differences between the present study and both Zieger et al. (2010)
616 and Silvergren et al. (2014) is probably related to the influence of large (>400 nm) particles in
617 determining κ based on aerosol optical properties and the bulk chemical composition.

618 Anttila et al. (2012) reported a κ value of approximately 0.1 at Pallas for the same period as
619 he presented activation diameters for (cf. Sect 3.3). The presented κ values are based on
620 HTDMA measurements at 90% relative humidity for particles with $D_d = 100$ nm. Jaatinen et
621 al. (2014) presented κ values obtained during the same measurement campaign as Anttila et
622 al. (2012). However, the hygroscopicity parameter was determined differently and for a
623 shorter period. The κ value derived by the critical diameter (cf. Sect 3.3) for a SS of 0.4% was
624 estimated to be approximately 0.1 and thus is in agreement with the HTDMA-based
625 observations of particles with $D_d = 100$ nm reported by Anttila et al. (2012). Conversely, the κ

626 calculated based on Aerosol Mass Spectrometer (AMS) data collected approximately 6
627 kilometres from the site of the CCN and HTDMA measurements was approximately 0.3. The
628 “CCN κ ” values determined in this study are higher than those obtained by Anttila et al.
629 (2012) and Jaatinen et al. (2014). These differences can be explained by the different
630 chemical composition of the aerosol population. Jaatinen et al. (2014) showed that at Pallas
631 47% of the measured mass concentration of the aerosols consisted of organic compounds,
632 while at Zeppelin 90% of the aerosol mass was inorganic material and thus more hygroscopic
633 material.

634 **4 Summary and Conclusions**

635 For the first time, size-resolved CCN measurements in the Arctic have been reported.
636 Measurements were conducted at the Zeppelin research station, Svalbard during two short
637 periods in June and August 2008. A near monodisperse aerosol having a D_p between 15 and
638 400 nm was selected by a DMA. The DMA was connected to a CCNC operating at 0.4% SS
639 and in parallel to a CPC 3010. Before and after the size-resolved CCN measurements were
640 taken, the CCNC was measuring the ambient air without previous selection of a monodisperse
641 aerosol. During these periods, the SS in the CCNC was changed to 0.2%, 0.4%, 0.6%, 0.8%
642 and 1%.

643 Trajectory analysis showed that during the measurement period in June 2008 air masses
644 arriving at Zeppelin were dominated by Arctic air, while during August 2008 air masses
645 originated from the Norwegian Sea and from the Barents Sea. A comparison of long-term
646 June particle number size distributions with those registered during the size-resolved CCN
647 measurements in June 2008 showed that the size distribution characterized by a nucleation
648 event and low particle concentrations for $D_p < 100$ nm is representative for averaged
649 conditions during June. In contrast, the particle number size distributions registered during
650 August 2008 indicate long-range transport that differs from the long-term observations during
651 August. In addition to the size-resolved CCN measurements, SS spectra were determined. In
652 June, this was done directly before the size-resolved measurements were completed and in
653 August directly before and after the size-resolved measurements were conducted. A power-
654 law function of the form $N_{ccn}(SS) = C * SS^k$, with N_{ccn} as the number of CCN and the
655 coefficients C and k , was fitted to the SS spectra. The coefficients for June were estimated to
656 be $C = 221$ and $k = 0.482$. Coefficients for August were $C = 251$ and $k = 0.367$ before the
657 size-resolved measurements were conducted and $C = 146$ and $k = 0.446$ after the size-

658 resolved measurements were conducted. The spectra measured during June lies between the
659 two measured during August. For a SS of 0.4%, CCN number concentrations as a function of
660 dry particle diameter were presented. From the size dependent CCN measurements, D_{50}
661 (particle diameter where $CCN/CN = 0.5$) was estimated. For the June 2008 measurement
662 period, D_{50} was 60 nm, while for the August 2008 measurement period, D_{50} was
663 approximately 67 nm. For the first time κ values for the Arctic were calculated based on
664 activation diameters obtained from in-situ size-resolved CCN measurements, meaning the κ
665 values are based on a conserved chemistry of the particles. Values of the hygroscopicity
666 parameter κ were calculated to be 0.4 and 0.3 for June and August, respectively. Estimating κ
667 based on simplified bulk chemical properties that were observed in June and August (2008)
668 gave a value of 0.5. The higher κ value based on chemistry is likely explained by an enhanced
669 influence of larger and more hygroscopic particles. It should be considered that, due to their
670 lower numbers, these larger particles are less crucial for CCN activation. Therefore, the κ
671 values based on in-situ measured size-resolved CCN measurements and growth factors are
672 probably more meaningful in characterizing the ability of an aerosol population to become
673 activated to cloud droplets. In future, it is needed to establish long term size-resolved CCN
674 measurements in the Arctic to study the size dependent activation of particles for different
675 seasons. An analysis of the difference in resulting κ values with κ values resulting from long-
676 term chemistry analysis of the particles is needed to quantify and explain the reason for the
677 differences and to point out possible differences to κ to the cloud model community.

678

679 **Acknowledgements**

680 We would like to thank Peter Tunved for providing the DMPS and CPC data. We
681 acknowledge that the CCN measurements were supported by the KOPRI project NRF-2011-
682 0021063. The authors gratefully acknowledge the NOAA Air Resources Laboratory (ARL)
683 for the provision of the HYSPLIT transport and dispersion model and the READY website
684 (<http://www.ready.noaa.gov>) used in this publication. The Swedish Environmental Protection
685 Agency (NV) is acknowledged for their financial support of measurements at the Zeppelin
686 station. We would like to point out that the NASA Micro-Pulse Lidar Network is funded by
687 the NASA Earth Observing System and Radiation Sciences Program. We thank the MPLNET
688 PI Masataka Shiobara and MPLNET staff Kerstin Binder for their efforts in establishing and

689 maintaining the Lidar measurements at Ny-Ålesund. The CRAICC project and the Bolin
690 Center for Climate Research are as well acknowledged.
691

692 References

- 693 Anttila, T., Vaattovaara, P., Komppula, M., Hyvärinen, A.-P., Lihavainen, H., Kerminen, V.-
694 M., and Laaksonen, A.: Size-dependent activation of aerosols into cloud droplets at a
695 subarctic background site during the second Pallas Cloud Experiment (2nd PaCE): method
696 development and data evaluation, *Atmos. Chem. Phys.*, 9, 4841-4854, 2009.
- 697 Anttila, T., Brus, D., Jaatinen, A., Hyvärinen, A.-P., Kivekäs, N., Romakkaniemi, S.,
698 Komppula, M., and Lihavainen, H.: Relationships between particles, cloud condensation
699 nuclei and cloud droplet activation during the third Pallas Cloud Experiment, *Atmos. Chem.*
700 *Phys.*, 12, 11435-11450, 2012.
- 701 Asa- Awuku, A., Nenes, A., Gao, S., Flagan, R. C., and Seinfeld, J. H.: Water- soluble SOA
702 from Alkene ozonolysis: composition and droplet activation kinetics inferences from analysis
703 of CCN activity, *Atmos. Chem. Phys.*, 10, 1585–1597, 2010.
- 704 Bhattu, D. and Tripathi, S. N.: Inter-seasonal variability in size-resolved CCN properties at
705 Kanpur, India, *Atmospheric Environment*, 85, 161–168, 2014.
- 706 Bigg, E. K. and Leck, C.: Cloud-active particles over the central Arctic Ocean, *J. Geophys.*
707 *Res.*, 106(D23), 32155-32166, 2001.
- 708 Boucher, O., Randall, D., Artaxo, P., Bretherton, C., Feingold, G., Forster, P., Kerminen, V.-
709 M., Kondo, Y., Liao, H., Lohmann, U., Rasch, P., Satheesh, S. K., Sherwood, S., Stevens, B.,
710 and Zhang, X. Y.: Clouds and Aerosols. In: *Climate Change 2013: The Physical Science*
711 *Basis. Contribution of Working Group I to the Fifth Assessment Report of the*
712 *Intergovernmental Panel on Climate Change [Stocker T.F., Qin D., Plattner G.-K., Tignor M.,*
713 *Allen S.K., Boschung J., Nauels A., Xia Y., Bex V. and Midgley P.M. (eds.)]. Cambridge*
714 *University Press, Cambridge, United Kingdom and New York, NY, USA*
- 715 Chang, R. Y.-W., Sjostedt, S. J., Pierce, J. R., Papakyriakou, T. N., Scarratt, M. G., Michaud,
716 S., Levasseur, M., Leitch, W. R., and Abbatt, J. P. D.: Relating atmospheric and oceanic
717 DMS levels to particle nucleation events in the Canadian Arctic, *J. Geophys. Res.*, 116,
718 D00S03, 2011.
- 719 Corrigan, C. E. and Novakov, T.: Cloud condensation nucleus activity of organic compounds:
720 a laboratory study, *Atmospheric Environment*, 33, 2661-2668, 1999.

721 Draxler, R. R. and Rolph, G. D.: HYSPLIT (HYbrid Single-Particle Lagrangian Integrated
722 Trajectory), 2014, Model access via NOAA ARL READY Website
723 (<http://ready.arl.noaa.gov/HYSPLIT.php>). NOAA Air Resources Laboratory, Silver Spring,
724 MD.

725 Ervens, B., Cubison, M. J., Andrews, E., Feingold, G., Ogren, J. A., Jimenez, J. L., Quinn, P.
726 K., Bates, T. S., Wang, J., Zhang, Q., Coe, H., Flynn, M., and Allan, J. D.: CCN predictions
727 using simplified assumptions of organic aerosol composition and mixing state: a synthesis
728 from six different locations, *Atmos. Chem. Phys.*, 10, 4795–4807, 2010.

729 Frosch, M., Prisle, N. L., Bilde, M., Varga, Z., and Kiss, G.: Joint effect of organic acids and
730 inorganic salts on cloud droplet activation, *Atmos. Chem. Phys.*, 11, 3895–3911, 2011.

731 Gunthe, S. S., King, S. M., Rose, D., Chen, Q., Roldin, P., Farmer, D. K., Jimenez, J. L.,
732 Artaxo, P., Andreae, M. O., Martin, S. T., and Pöschl, U.: Cloud condensation nuclei in
733 pristine tropical rainforest air of Amazonia: size-resolved measurements and modeling of
734 atmospheric aerosol composition and CCN activity, *Atmos. Chem. Phys.*, 9, 7551-7575,
735 2009.

736 Hegg, D. A., Ferek, R. J., and Hobbs, P. V.: Cloud Condensation Nuclei over the Arctic
737 Ocean in Early Spring, *J. Appl. Meteor.*, 34, 2076-2082, 1995.

738 Hegg, D. A., Hobbs, P. V., Gassó, S., Nance, J. D., and Rangno, A. L.: Aerosol measurements
739 in the Arctic relevant to direct and indirect radiative forcing, *J. Geophys. Res.*, 101(D18),
740 23349-23363, 1996.

741 Hiranuma, N., Brooks, S. D., Moffet, R. C., Glen, A., Laskin, A., Gilles, M. K., Liu, P.,
742 Macdonald, A. M., Strapp, J. W., and McFarquhar, G. M.: Chemical characterization of
743 individual particles and residuals of cloud droplets and ice crystals collected on board
744 research aircraft in the ISDAC 2008 study, *J. Geophys. Res. Atmos.*, 118, 6564-6579, 2013.

745 Hoppel, W. A., Dinger, J. E., and Ruskin, R. E.: Vertical Profiles of CCN at Various
746 Geographical Locations, *J. Atmos. Sci.*, 30, 1410-1420, 1973.

747 Jaatinen, A., Romakkaniemi, S., Anttila, T., Hyvärinen, A.-P., Hao, L.-Q., Kortelainen, A.,
748 Miettinen, P., Mikkonen, S., Smith, J. N., Virtanen, A., and Laaksonen, A.: The third Pallas

749 Cloud Experiment: Consistency between the aerosol hygroscopic growth and CCN activity,
750 *Boreal Env. Res.* 19 (suppl. B), 368-382, 2014.

751 Komppula, M., Lihavainen, H., Hatakka, J., Paatero, J., Aalto, P., Kulmala, M., and Viisanen,
752 Y.: Observations of new particle formation and size distributions at two different heights and
753 surroundings in subarctic area in northern Finland, *J. Geophys. Res.*, 108, 4295, D9, 2003.

754 Komppula, M., Lihavainen, H., Kerminen, V.-M., Kulmala, M., and Viisanen, Y.:
755 Measurements of cloud droplet activation of aerosol particles at a clean subarctic background
756 site, *J. Geophys. Res.*, 110, D06204, 2005.

757 Kreidenweis, S. M., Koehler, K., DeMott, P. J., Prenni, A. J., Carrico, C., and Ervens, B.:
758 Water activity and activation diameters from hygroscopicity data—Part I: Theory and
759 application to inorganic salts, *Atmos. Chem. Phys.*, 5, 1357-1370, 2005.

760 Kuang, C., McMurry, P. H., McCormick, A. V., and Eisele, F. L.: Dependence of nucleation
761 rates on sulfuric acid vapor concentration in diverse atmospheric locations, *J. Geophys. Res.*,
762 113, D10209, 2008.

763 Kulmala, M., Kontkanen, J., Junninen, H., Lehtipalo, K., Manninen, H. E., Nieminen, T.,
764 Petäjä, T., Sipilä, M., Schobesberger, S., Rantala, P., Franchin, A., Jokinen, T., Järvinen, E.,
765 Äijälä, M., Kangasluoma, J., Hakala, J., Aalto, P. P., Paasonen, P., Mikkilä, J., Vanhanen, J.,
766 Aalto, J., Hakola, H., Makkonen, U., Ruuskanen, T., Mauldin, III R. L., Duplissy, J.,
767 Vehkamäki, H., Bäck, J., Kortelainen, A., Riipinen, I., Kurtén, T., Johnston, M. V., Smith, J.
768 N., Ehn, M., Mentel, T. F., Lehtinen, K. E. J., Laaksonen, A., Kerminen, V.-M., Worsnop, D.
769 R.: Direct Observations of Atmospheric Aerosol Nucleation, *Science*, 339, 943-946, 2013.

770 Kumar, P. P., Broekhuizen, K., and Abbatt, J. P. D.: Organic acids as cloud condensation
771 nuclei: Laboratory studies of highly soluble and insoluble species, *Atmos. Chem. Phys.*, 3,
772 509-520, 2003.

773 Latham, T. L., Beyersdorf, A. J., Thornhill, K. L., Winstead, E. L., Cubison, M. J., Hecobian,
774 A., Jimenez, J. L., Weber, R. J., Anderson, B. E., and Nenes, A.: Analysis of CCN activity of
775 Arctic aerosol and Canadian biomass burning during summer 2008, *Atmos. Chem. Phys.*, 13,
776 2735-2756, 2013.

777 Martin, M., Chang, R. Y.-W., Sierau, B., Sjogren, S., Swietlicki, E., Abbatt, J. P. D., Leck, C.,
778 and Lohmann, U.: Cloud condensation nuclei closure study on summer arctic aerosol, *Atmos.*
779 *Chem. Phys.*, 11, 11335-11350, 2011.

780 Moore, R. H., Bahreini, R., Brock, C. A., Froyd, K. D., Cozic, J., Holloway, J. S.,
781 Middlebrook, A. M., Murphy, D. M., and Nenes, A.: Hygroscopicity and composition of
782 Alaskan Arctic CCN during April 2008, *Atmos. Chem. Phys.*, 11, 11807-11825, 2011a.

783 Moore, M. J. K., Furutani, H., Roberts, G. C., Moffet, R. C., Gilles, M. K., Palenik, B., and
784 Prather, K. A.: Effect of organic compounds on cloud condensation nuclei (CCN) activity of
785 sea spray aerosol produced by bubble bursting, *Atmospheric Environment*, 45, 7462-7469,
786 2011b.

787 Ortega, I. K., Suni, T., Boy, M., Grönholm, T., Manninen, H. E., Nieminen, T., Ehn, M.,
788 Junninen, H., Hakola, H., Hellén, H., Valmari, T., Arvela, H., Zegelin, S., Hughes, D.,
789 Kitchen, M., Cleugh, H., Worsnop, D. R., Kulmala, M., and Kerminen, V.-M.: New insights
790 into nocturnal nucleation, *Atmos. Chem. Phys.*, 12, 4297-4312, 2012.

791 Paramonov, M., Aalto, P. P., Asmi, A., Prisle, N., Kerminen, V.-M., Kulmala, M., and Petäjä,
792 T.: The analysis of size-segregated cloud condensation nuclei counter (CCNC) data and its
793 implications for cloud droplet activation, *Atmos. Chem. Phys.*, 13, 10285-10301, 2013.

794 Park, K., Kim, G., Kim, J.-s., Yoon, Y.-J., Cho, H.-j., and Ström, J.: Mixing State of Size-
795 Selected Submicrometer Particles in the Arctic in May and September 2012, *Environ. Sci.*
796 *Technol.*, 48, 909-919, 2014.

797 Petters, M. D. and Kreidenweis, S. M.: A single parameter representation of hygroscopic
798 growth and cloud condensation nucleus activity, *Atmos. Chem. Phys.*, 7, 1961–1971, 2007.

799 Pruppacher, H. R. and Klett, J. D.: *Microphysics of Clouds and Precipitation*, Atmospheric
800 and Oceanographic Sciences Library, Volume 18, ISBN 9780306481000, Dordrecht: Springer
801 Netherlands, (copyright 2010).

802 Rastak, N., Silvergren, S., Zieger, P., Wideqvist, U., Ström, J., Svenningsson, B., Maturilli,
803 M., Tesche, M., Ekman, A.M.L., Tunved, P., and Riipinen, I.: Seasonal variation of aerosol
804 water uptake and its impact on the direct radiative effect at Ny-Ålesund, Svalbard, *Atmos.*
805 *Chem. Phys.*, 14, 7445-7460, 2014.

806 Riipinen, I., Sihto, S.-L., Kulmala, M., Arnold, F., Dal Maso, M., Birmili, W., Saarnio, K.,
807 Teinilä, K., Kerminen, V.-M., Laaksonen, A., and Lehtinen, K. E. J.: Connections between
808 atmospheric sulphuric acid and new particle formation during QUEST III–IV campaigns in
809 Heidelberg and Hyytiälä, *Atmos. Chem. Phys.*, 7, 1899-1914, 2007.

810 Rogers, R. R. and Yau, M. K.: A Short Course in Cloud Physics, 3rd edition, International
811 Series in Natural Philosophy, 113, Butterworth-Heinemann an imprint of Elsevier, ISBN 0-
812 7506-3215-1, (1996 reprint).

813 Rolph, G. D.: Real-time Environmental Applications and Display sYstem (READY) Website
814 (<http://ready.arl.noaa.gov>). NOAA Air Resources Laboratory, Silver Spring, MD, 2014.

815 Rose, D., Nowak, A., Achtert, P., Wiedensohler, A., Hu, M., Shao, M., Zhang, Y., Andreae,
816 M. O., and Pöschl, U.: Cloud condensation nuclei in polluted air and biomass burning smoke
817 near the mega-city Guangzhou, China–Part 1: Size-resolved measurements and implications
818 for the modeling of aerosol particle hygroscopicity and CCN activity, *Atmos. Chem. Phys.*,
819 10, 3365-3383, 2010.

820 Shaw, G. E.: Cloud condensation nuclei associated with Arctic haze, *Atmospheric*
821 *Environment*, 20, 1453-1456, 1986.

822 Silvergren, S. Wideqvist, U., Ström, J., Sjogren, S., and Svenningsson, B.: Hygroscopic
823 growth and cloud forming potential of Arctic aerosol based on observed chemical and
824 physical characteristics (a 1 year study 2007-2008), *J. Geophys. Res. Atmos*, 119, 14,080-
825 14,097, 2014.

826 Sipilä, M., Berndt, T., Petäjä, T., Brus, D., Vanhanen, J., Stratmann, F., Patokoski, J.,
827 Mauldin, III R. L., Hyvärinen, A.-P., Lihavainen, H., and Kulmala, M.: The Role of Sulfuric
828 Acid in Atmospheric Nucleation, *Science*, 327, 1243-1246, 2010.

829 Sullivan, R. C., Moore, M. J. K., Petters, M. D., Kreidenweis, S. M., Roberts, G. C., and
830 Prather, K. A.: Effect of chemical mixing state on the hygroscopicity and cloud nucleation
831 properties of calcium mineral dust particles, *Atmos. Chem. Phys.*, 9, 3303-3316, 2009.

832 Tunved, P., Ström, J., and Krejci, R.: Arctic aerosol life cycle: linking aerosol size
833 distributions observed between 2000 and 2010 with air mass transport and precipitation at
834 Zeppelin station, Ny-Ålesund, Svalbard, *Atmos. Chem. Phys.*, 13, 3643-3660, 2013.

835 Yli-Juuti, T., Nieminen, T., Hirsikko, A., Aalto, P. P., Asmi, E., Hörrak, U., Manninen, H. E.,
836 Patokoski, J., Dal Maso, M., Petäjä, T., Rinne, J., Kulmala, M., and Riipinen, I.: Growth rates
837 of nucleation mode particles in Hyytiälä during 2003–2009: variation with particle size,
838 season, data analysis method and ambient conditions, *Atmos. Chem. Phys.*, 11, 12865-12886,
839 2011.

840 Yum, S. S. and Hudson, J. G.: Vertical distributions of cloud condensation nuclei spectra over
841 the springtime Arctic Ocean, *J. Geophys. Res.*, 106(D14), 15045-15052, 2001.

842 Zieger, P., Fierz-Schmidhauser, R., Gysel, M., Ström, J., Henne, S., Yttri, K. E.,
843 Baltensperger, U., and Weingartner, E.: Effects of relative humidity on aerosol light scattering
844 in the Arctic, *Atmos. Chem. Phys.*, 10, 3875-3890, 2010.

845

846 Table 1. Measured diameters when $CCN/CN = 0.25, 0.50$ and 0.75 and corresponding
 847 calculated κ values with Eq. (1)

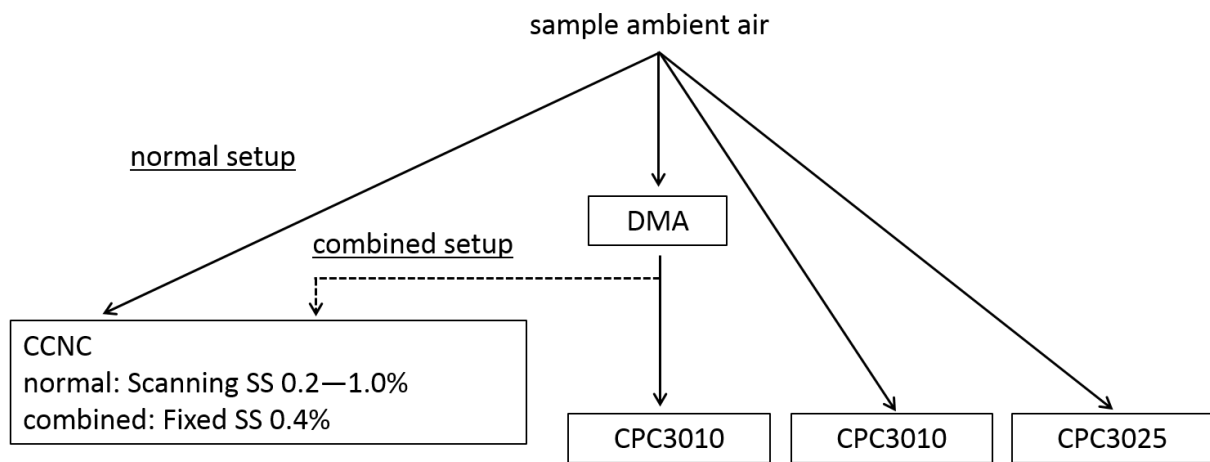
	June		August	
	Activation diameter (nm)	κ	Activation diameter (nm)	κ
CCN/CN = 0.25	49	0.7	56	0.5
CCN/CN = 0.50	60	0.4	67	0.3
CCN/CN = 0.75	72	0.2	78	0.2

848

849 Table 2. Experimentally-derived mass fractions (Silvergren et al., 2014), densities ρ and κ_i
 850 values for each component used for the total κ calculations (Rastak et al., 2014 and references
 851 therein). Properties of ammonium sulphate were assumed for the inorganic fraction.

Component	Mass fraction (%)	Mass fraction (%)	ρ (kg m ⁻³)	κ_i
	June	August		
inorganics	88	90	1770	0.53
more water-soluble organics	10	7	1560	0.27
less water-soluble organics	2	2	1500	0.10
elemental carbon	1	1	1800	0.00
				Total κ
	June			0.5
	August			0.5

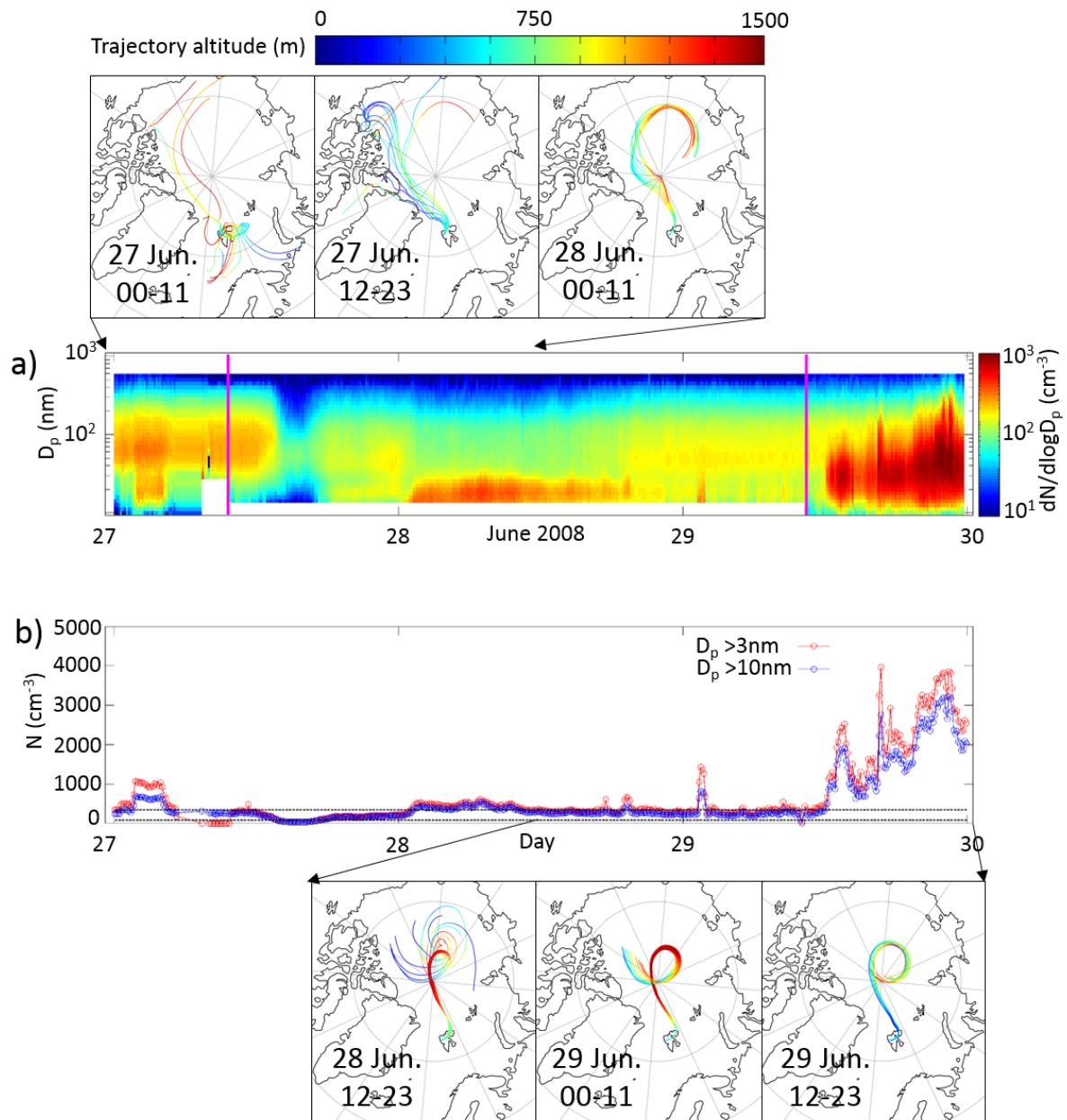
852



854

855 Figure 1. Scheme of the two different measurement modes for the cloud condensation nuclei
 856 counter (CCNC). When CCN size-resolved number concentration measurements took place,
 857 the CCNC was connected behind the Differential Mobility Analyzer and the supersaturation
 858 was set to 0.4%. During normal operation, the CCNC was connected parallel to the DMA and
 859 SS alternated between 0.2% and 1.0%.

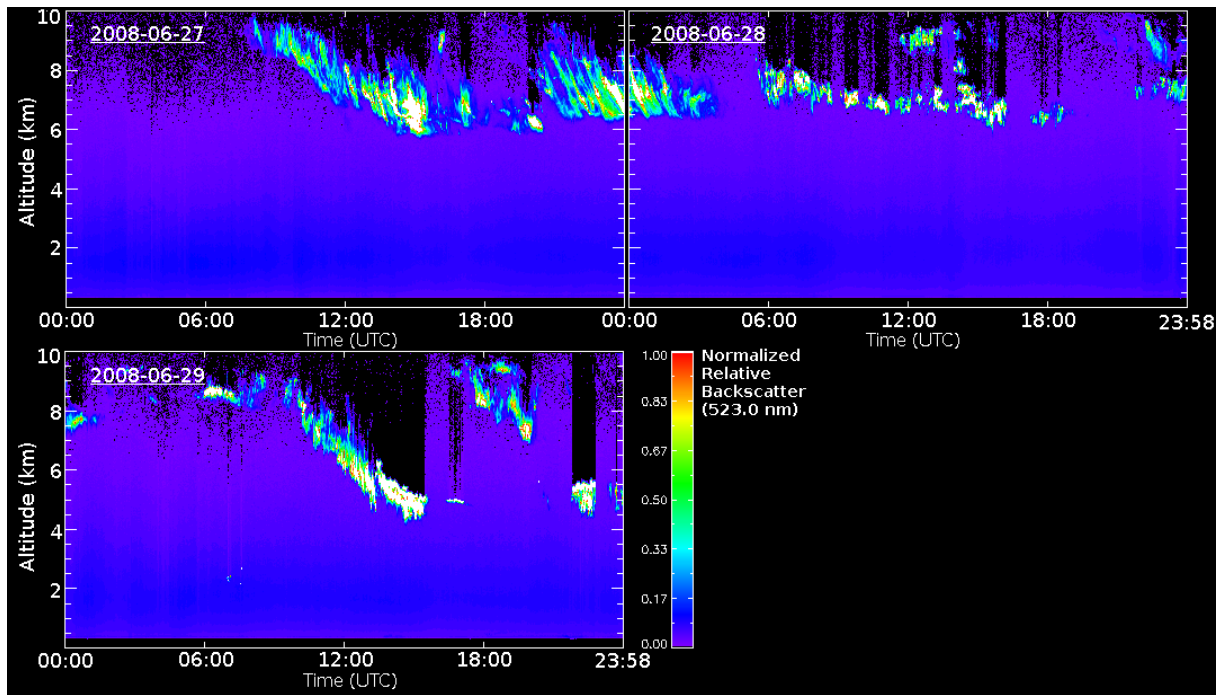
860



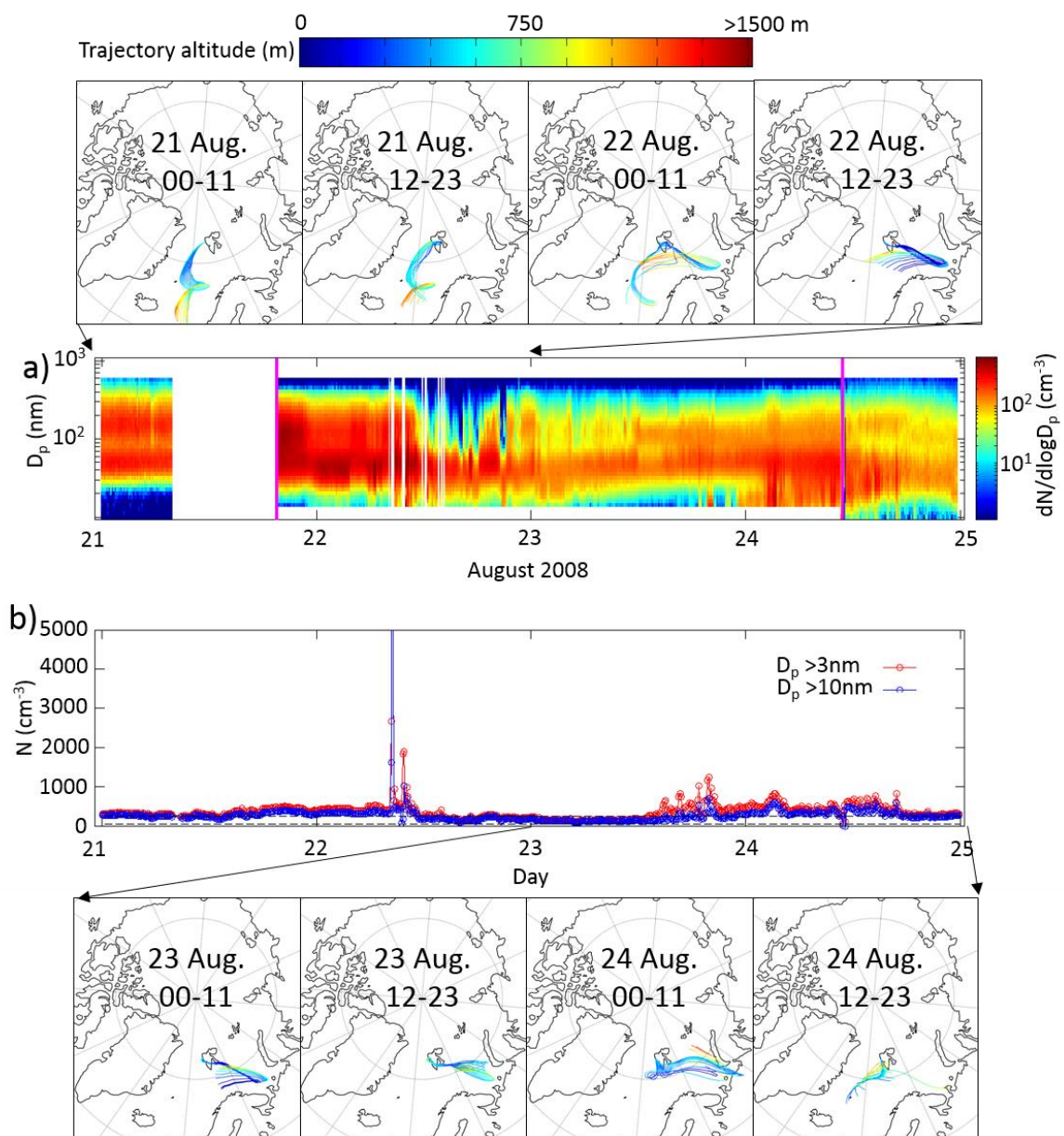
861

862 Figure 2. a) Particle number size concentration measured before, during, and after the size-
 863 size-resolved CCN concentration measurements were conducted in June 2008. Purple vertical lines
 864 indicate the start and end time of the CCN size-resolved concentration measurements. b) Time
 865 series of the 8-min medians from CPC measurements for the same period in June 2008.
 866 Horizontal dashed lines represent the 25th and 75th percentile of the CN number concentration
 867 for June during the years 2001 to 2010. Trajectory plots show 5-day backward trajectories,
 868 calculated for every hour. Trajectory plots on top of panel a) show air masses arriving
 869 between the 27 and midday of the 28 June at Zeppelin Research Station. Trajectory plots

870 below panel b) show air masses arriving between midday of the 28 June to midnight of the 29
871 June at Zeppelin Research Station.
872



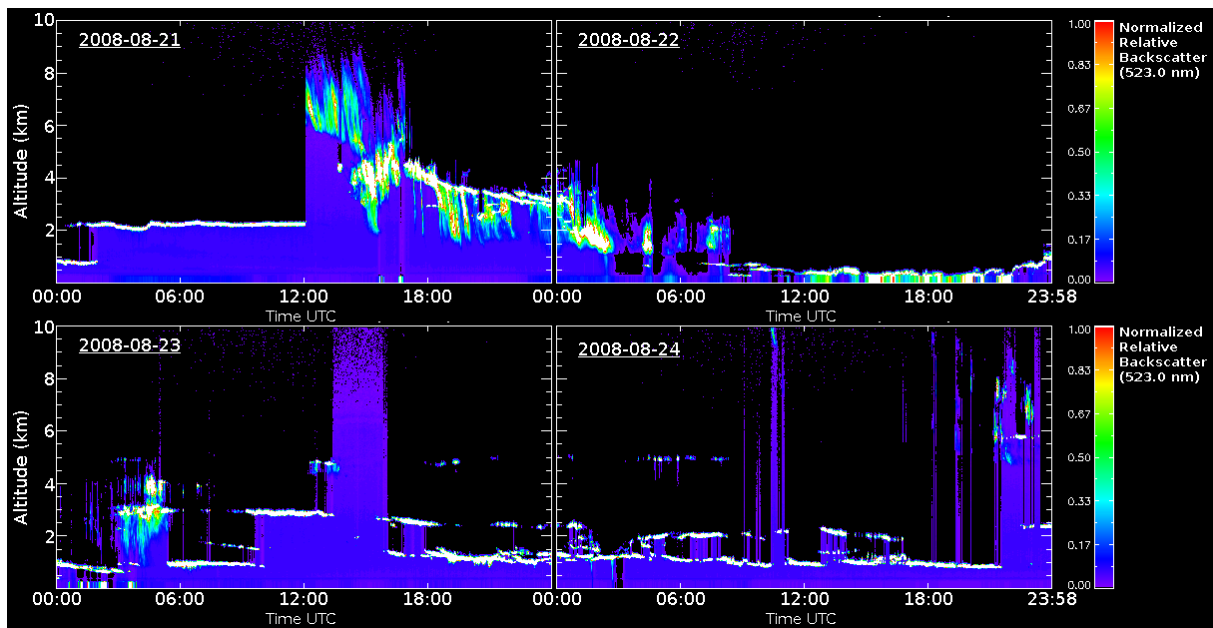
873
 874 Figure 3. Normalized relative backscatter (Level 1.0 data) based on Lidar measurements at
 875 Ny-Ålesund recorded during the period 27–29 June 2008 (modified from
 876 <http://mplnet.gsfc.nasa.gov/>)



877

878 Figure 4. a) Particle number size concentration measured before, during, and after the size-
 879 resolved CCN concentration measurements were conducted in August 2008. Purple vertical
 880 lines indicate the start and end time of the CCN size-resolved concentration measurements. b)
 881 Time series of the 8-min medians from CPC measurements for the same period in August
 882 2008. Horizontal dashed lines represent the 25th and 75th percentile of the CN number
 883 concentration for August during the years 2001 to 2010. Trajectory plots show 5-day
 884 backward trajectories, calculated for every hour. Trajectory plots on top of panel a) show air
 885 masses arriving between the 21 and 23 August 2008 at Zeppelin Research Station. Trajectory
 886 plots below panel b) show air masses arriving between midnight of the 23 August to midnight
 887 of the 24 August at Zeppelin Research Station.

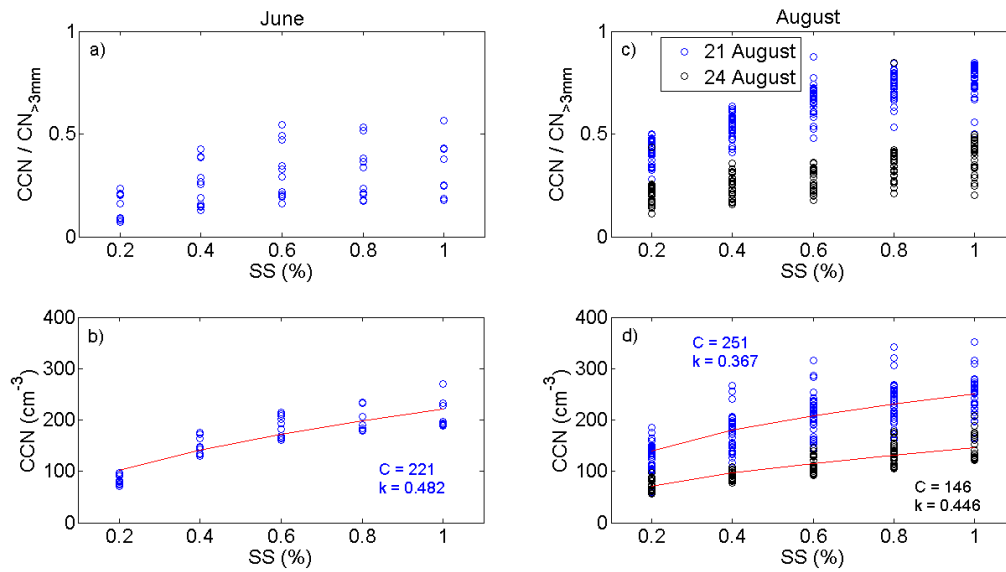
888



889

890 Figure 5. Normalized relative backscatter (Level 1.0 data) based on Lidar measurements at
 891 Ny-Ålesund recorded during the period 21–24 August 2008 (modified from
 892 <http://mplnet.gsfc.nasa.gov/>)

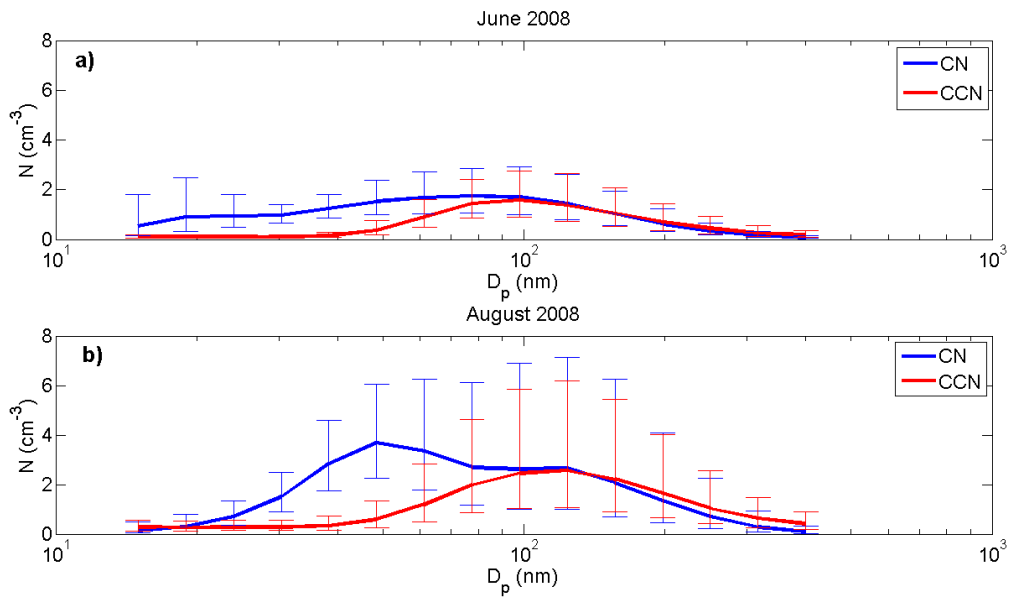
893



894

895 Figure 6. a) Ratios of the medians for each SS scan between CCN and particles with
 896 diameters $> 3\text{nm}$ ($\text{CN}_{>3\text{nm}}$) for June 2008 as a function of SS. b) Medians for each SS scan of
 897 the total numbers of CCN as a function of SS for June 2008. c) Ratios of the medians for each
 898 SS scan between CCN and particles with diameters $> 3\text{nm}$ ($\text{CN}_{>3\text{nm}}$) for 21 and 24 August
 899 2008 as a function of SS. d) Medians for each SS scan of the total numbers of CCN as a
 900 function of SS for 21 and 24 August 2008. The red curves represent power-law function fits
 901 to the data with the coefficients C and k .

902

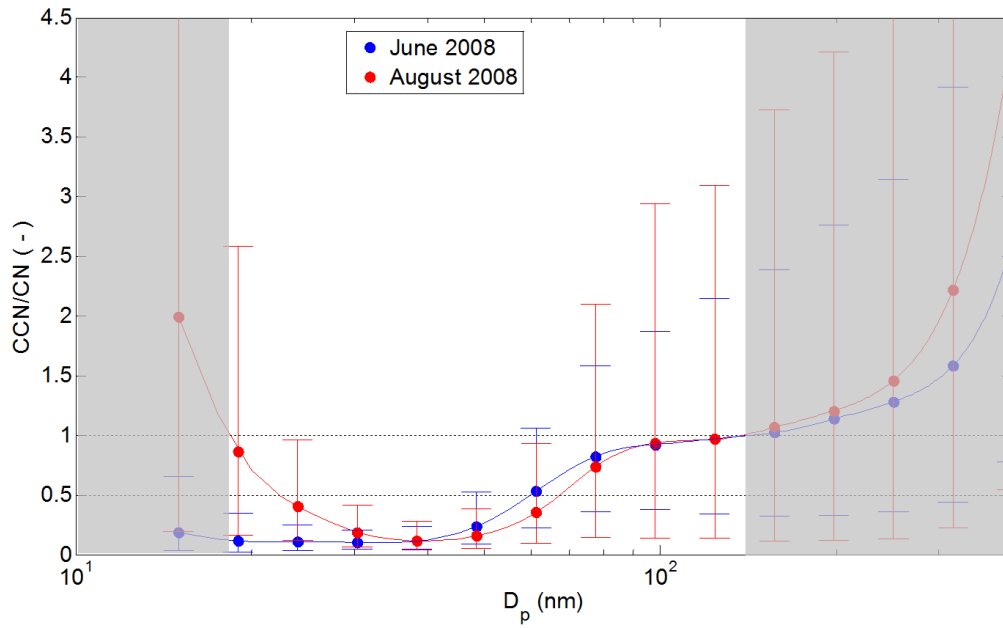


903

904 Figure 7. Geometric means of size-resolved particle density measurements and resulting CCN
 905 concentrations for the measurement period in a) June 2008 and b) August 2008.

906 Measurements were conducted at 0.4% SS. Error bars indicate the geometric standard
 907 deviation.

908



909

910 Figure 8. Activation ratio as a function of dry particle diameter (D_p) for the measurement

911 period in June 2008 and August 2008. Obtained from measurements at a SS of 0.4%. Error

912 bars indicate SD. The grey area indicates the for further analysis omitted data.